BULLETIN *of the*
MALAYSIAN MATHEMATICAL
SCIENCES SOCIETY
http://math.usm.my/bulletin

Bull. Malays. Math. Sci. Soc. (2) **37***(1) (2014), 1–24*

Numerical Evaluation of Conformal Mapping and its Inverse for Unbounded Multiply Connected Regions

[1]ARIF A. M. YUNUS, [2]ALI H. M. MURID AND [3]MOHAMED M. S. NASSER
[1]Faculty of Science and Technology, Universiti Sains Islam Malaysia,
71800, Bandar Baru Nilai, Negeri Sembilan, Malaysia
[2]UTM Centre of Industrial and Applied Mathematics (UTM-CIAM), Universiti Teknologi Malaysia,
81310 UTM Johor Bahru, Johor, Malaysia
Department of Mathematical Sciences, Faculty of Science, Universiti Teknologi Malaysia,
81310 UTM Johor Bahru, Johor, Malaysia
[3]Department of Mathematics, Faculty of Science, Ibb University, P. O. Box 70270, Ibb, Yemen
Department of Mathematics, Faculty of Science, King Khalid University,
P. O. Box 9004, Abha, Saudi Arabia
[1]arifasraf@hotmail.com, [2]alihassan@utm.my, [3]mms_nasser@hotmail.com

Abstract. A boundary integral equation method for numerical evaluation of the conformal mapping and its inverse from unbounded multiply connected regions onto five canonical slit regions is presented in this paper. This method is based on a uniquely solvable boundary integral equation with the adjoint generalized Neumann kernel. This method is accurate and reliable. Some numerical examples are presented to illustrate the effectiveness of this method.

2010 Mathematics Subject Classification: Primary 30C30, 30E25, 65E05

Keywords and phrases: Numerical conformal mapping, unbounded multiply connected regions, boundary integral equation, adjoint generalized Neumann kernel.

1. Introduction

In this paper, we present a unified method for univalent conformal mapping and its inverse of unbounded multiply connected regions onto five canonical slit regions. Conformal mapping plays an important role in the fields of sciences and engineering. Applications of conformal slit maps in applied mathematics, e.g., point vortices and sources in ideal flow, Hele-Shaw flows or Laplacian growth problems and hollow vortices have been reviewed recently in [7].

Exact conformal maps are known only for certain regions. Therefore, numerous researchers have applied numerical method to overcome this limitation. Trefethen [30] has discussed several methods for computing conformal mapping numerically. Generally, these methods are based on expansion methods, iterative methods and integral equation methods.

There exist several classes of canonical regions with regards to conformal mapping of multiply connected regions as listed in [3, 14, 15, 24, 34]. The famous five canonical regions

Communicated by Rosihan M. Ali, Dato'.
Received: January 3, 2013; *Revised:* April 11, 2013.

are: disk with circular slits region U_d, annulus with circular slits region U_a, circular slits region U_c, radial slits region U_r, and parallel slits region U_p. These classes of canonical regions have been studied by several authors for the cases of bounded or unbounded multiply connected regions (see [1, 2, 6, 9, 10, 25–29, 32, 35]).

The multiply connected circular region (a region all of whose boundaries are circles) is itself a canonical region region for conformal mapping of multiply connected regions (see [5, 6, 9–11, 14, 31, 32]). Wegmann method [31] and Fornberg-like methods [5, 6] are examples of iterative methods which can be used for computing the conformal mapping from multiply connected circular regions to multiply connected region whose boundaries are smooth curves (see also [12, 32]). Analytical formulae for the mapping of bounded multiply connected circular region onto the canonical class mentioned above have been given in [9]. These mapping functions were found in terms of a special function called the Schottky-Klein prime function. Crowdy [8] used also the Schottky-Klein prime function to give analytical formulae, dependent on just a finite set of so-called accessory parameters, for the conformal mapping from a circular multiply connected domain to a bounded multiply connected polygon. Crowdy's formula (see [8, Equation(1.1)]) is the natural extension of the classical Schwarz-Christoffel formula to a simply connected polygon.

Amano [1] have successfully mapped unbounded multiply connected regions onto circular slit regions and radial slit regions by means of charge simulation methods. Nasser [17,18] managed to map bounded and unbounded multiply connected regions onto these five canonical regions by reformulating the mapping function as a Riemann-Hilbert problem which is solved by means of boundary integral equation with the generalized Neumann kernel. The right-hand side of the integral equation involves integral with cotangent singularity which is approximated by Wittich's method. The integral equation was discretized by the Nyström method with the trapezoidal rule to obtain a dense and non-symmetric linear system. The obtained linear system was solved in [17, 18] using the Gauss elimination method of order $O((mn)^3)$ operations where m is the multiplicity of the multiply connected region and n is the number of nodes in the discretization of each boundary components. Hence, it is impossible to solve the linear system for large values of m and n. In the recent paper [19], the linear system is solved using the generalized minimum residual (GMRES) method powered by the fast multipole method (FMM). The new solution procedure requires only $O(mn\ln n)$ operations. This gives the authors in [19] a fast method of boundary integral equation with the generalized Neumann kernel to compute conformal mapping of multiply connected regions of high connectivity.

The approach used in [17, 18] has been used by Nasser *et al.* [20] to derive a boundary integral equation with the adjoint generalized Neumann kernel to compute numerically the conformal mapping and its inverse from bounded multiply connected regions onto the above five canonical slit regions. The boundary integral equation with the adjoint generalized Neumann kernel has been derived by reformulating the mapping function as an adjoint Riemann-Hilbert problem.

Murid and Hu [16] managed to map a bounded multiply connected region onto a unit disk with slits via boundary integral equation method. However, the integral equation involves unknown conformal moduli which lead to a system of nonlinear algebraic equation upon discretization of the integral equation. Sangawi *et al.* [25–29] managed to overcome this nonlinearity problem and later extended [16] work for numerical conformal mapping of bounded multiply connected regions onto the above five canonical slit regions. Recently,

Yunus *et al.* [35] managed to extend Sangawi *et al.* method [16, 25–29] to unbounded multiply connected regions onto the above five canonical slit regions in a unified way. This method is based on solving three linear integral equations separately before one can approximate the boundary values of the mapping function. These boundary integral equations are constructed from a boundary relationship satisfied by an analytic function on an unbounded multiply connected region.

In this paper, we present a new method for approximating numerical conformal mapping of unbounded multiply connected regions onto the above five canonical slit regions and its inverse mapping in a unified way via a boundary integral equation with the adjoint generalized Neumann kernel. Only the right-hand side of the integral equation is different from a canonical region to another. The plan of this paper is as follows: Section 2 presents some notations and auxiliary materials. Section 3 presents a method for finding an unknown function $S(t)$ in connection with conformal mapping. In Sections 4–8, we present the derivation for numerical conformal mapping for all five types of canonical regions. In Section 9, we give some examples to illustrate the effectiveness of our method. Finally, Section 10 presents a short conclusion.

2. Notations and auxiliary materials

Let Ω^- be an unbounded multiply connected region of connectivity m. The boundary Γ consists of m smooth Jordan curves Γ_j, $j = 1,2,\ldots,m$ i.e., $\Gamma = \Gamma_1 \cup \Gamma_2 \cup \cdots \cup \Gamma_m$. The boundaries Γ_j are assumed to be in clockwise orientation (see Figure 1). The curve Γ_j is parameterized by 2π-periodic twice continuously differentiable complex function $\eta_j(t)$ with non-vanishing first derivative, i.e.,

$$\eta_j'(t) = \frac{d\eta_j(t)}{dt} \neq 0, \quad t \in J_j = [0,2\pi], \quad k = 1,\ldots,m.$$

The total parameter domain J is the disjoint union of m intervals $J_1,\ldots,J_m$. We define a parameterization η of the whole boundary Γ on J by

$$\eta(t) = \begin{cases} \eta_1(t), & t \in J_1 = [0,2\pi], \\ \quad \vdots & \\ \eta_m(t), & t \in J_m = [0,2\pi]. \end{cases} \tag{2.1}$$

Let $\Phi(z)$ be the conformal mapping function that maps Ω^- onto U^- , where U^- represents any of the canonical regions mentioned above, z_j is a prescribed point located inside Γ_j, $j = 1,2,\ldots,m$ and β is prescribed point located in Ω^-. In this paper, we determine the mapping function $\Phi(z)$ by computing two unknown real functions on J, a function $S(t)$ and a piecewise constant real function $R(t)$. Let H be the space of all real Hölder continuous 2π -periodic function and L be the subspace of H which contains the piecewise real constant functions $R(t)$. The unknown function $S(t)$ for the function $\Phi(z)$ shall be written as

$$S(t) = \begin{cases} S_1(t), & t \in J_1, \\ \quad \vdots & \\ S_m(t), & t \in J_m. \end{cases} \tag{2.2}$$

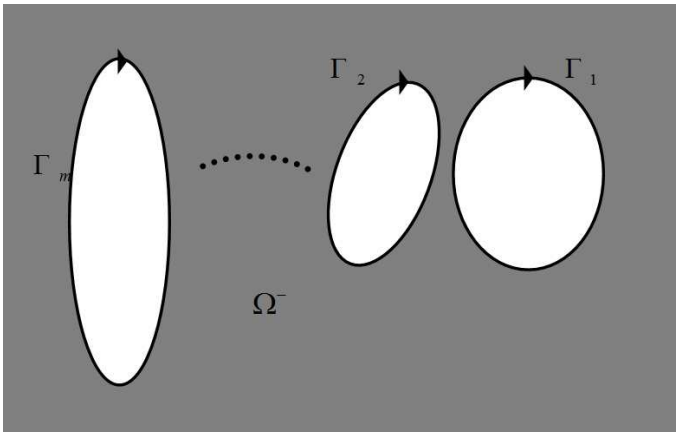

Figure 1. An unbounded multiply connected region Ω^- with connectivity m

The piecewise constant real function $R(t)$ is written as

$$R(t) = \begin{cases} R_1, & t \in J_1, \\ \vdots & \\ R_m, & t \in J_m, \end{cases} \tag{2.3}$$

or briefly written as $R(t) = (R_1, \ldots, R_m)$. Let $A(t)$ be a complex continuously differentiable 2π-periodic function for all $t \in J$. We define two real kernels formed with A as [33]

$$N(s,t) = \frac{1}{\pi}\mathrm{Im}\left(\frac{A(s)}{A(t)}\frac{\eta'(t)}{\eta(t)-\eta(s)}\right),$$

$$M(s,t) = \frac{1}{\pi}\mathrm{Re}\left(\frac{A(s)}{A(t)}\frac{\eta'(t)}{\eta(t)-\eta(s)}\right).$$

The kernel $N(s,t)$ is known as the generalized Neumann kernel formed with a complex-function A and η. The kernel $N(s,t)$ is continuous with

$$N(t,t) = \frac{1}{\pi}\mathrm{Im}\left(\frac{1}{2}\frac{\eta''(t)}{\eta'(t)} - \frac{A'(t)}{A(t)}\right).$$

The kernel $M(s,t)$ has a cotangent singularity

$$M(s,t) = -\frac{1}{2\pi}\cot\frac{s-t}{2} + M_1(s,t),$$

where, the kernel $M_1(s,t)$ is continuous with

$$M_1(t,t) = \frac{1}{\pi}\mathrm{Re}\left(\frac{1}{2}\frac{\eta''(t)}{\eta'(t)} - \frac{A'(t)}{A(t)}\right).$$

The adjoint function $\tilde{A}$ of A is defined by

$$\tilde{A} = \frac{\eta'(t)}{A(t)}. \tag{2.4}$$

Then the generalized Neumann kernel $\tilde{N}(s,t)$ and the real kernel $\tilde{M}$ formed with $\tilde{A}$ is defined by

$$\tilde{N}(s,t) = \frac{1}{\pi}\mathrm{Im}\left(\frac{\tilde{A}(s)}{\tilde{A}(t)}\frac{\eta'(t)}{\eta(t)-\eta(s)}\right), \tag{2.5}$$

$$\tilde{M}(s,t) = \frac{1}{\pi}\mathrm{Re}\left(\frac{\tilde{A}(s)}{\tilde{A}(t)}\frac{\eta'(t)}{\eta(t)-\eta(s)}\right). \tag{2.6}$$

Then,

$$\tilde{N}(s,t) = -N^*(s,t) \quad \text{and} \quad \tilde{M}(s,t) = -M^*(s,t), \tag{2.7}$$

where $N^*(s,t) = N(t,s)$ is the adjoint kernel of the generalized Neumann kernel $N(s,t)$. We define the Fredholm integral operators $\mathbf{N}^*$ by

$$\mathbf{N}^*\upsilon(t) = \int_J N^*(t,s)\upsilon(s)ds, \qquad t \in J.$$

Throughout this paper, we shall assume the function A and $\tilde{A}$ are given by

$$A(t) = 1 \qquad \text{and} \qquad \tilde{A}(t) = \eta'(t). \tag{2.8}$$

It is known that $\lambda = 1$ is not an eigenvalue of the kernel N and $\lambda = -1$ is an eigenvalue of the kernel N with multiplicity m [33]. The eigenfunctions of N corresponding to the eigenvalue $\lambda = -1$ are $\left\{\chi^{[1]}, \chi^{[2]}, \ldots, \chi^{[m]}\right\}$, where

$$\chi^{[j]}(\xi) = \begin{cases} 1, & \xi \in \Gamma_j, \\ 0, & \text{otherwise}, \end{cases} \quad j = 1,2,\ldots,m.$$

We also define an integral operator $\mathbf{J}$ by (see [25])

$$\mathbf{J}\mu(s) := \int_J \frac{1}{2\pi}\sum_{j=1}^{m}\chi^{[j]}(s)\chi^{[j]}(t)\mu(t)dt. \tag{2.9}$$

The following theorem [20] gives us a method for calculating the piecewise constant real function $h(t)$ in connection with conformal mapping later. The proof of this theorem is reproduced for convenience.

Theorem 2.1. *Let $\gamma, \mu \in H$ and $h, \nu \in L$ such that*

$$Af = \gamma + h + \mathrm{i}[\mu + \nu] \tag{2.10}$$

are boundary values of a function $f(z)$ analytic in Ω^- with $f(\infty) = 0$. Then the functions $h = (h_1, h_2, \ldots, h_m)$ and $\nu = (\nu_1, \nu_2, \ldots, \nu_m)$ have each element given by

$$h = \sum_{k=1}^{m}\left(\gamma, \vartheta^{[k]}\right)\chi^{[k]}, \tag{2.11}$$

$$\nu = \sum_{k=1}^{m}\left(\mu, \vartheta^{[k]}\right)\chi^{[k]}, \tag{2.12}$$

where $\vartheta^{[k]}$ is the unique solution of the integral equation

$$(\mathbf{I} + \mathbf{N}^* + \mathbf{J})\vartheta^{[k]} = -\chi^{[k]}, \quad k = 1,2,\ldots,m. \tag{2.13}$$

Proof. Formula (2.11) is an extension of [21, Theorem 5]. For (2.12), the function $\hat{f}(z) := -\mathrm{i}f(z)$ is analytic in Ω^- with $\hat{f}(\infty) = 0$ and has the boundary values

$$A\hat{f} = \mu + \nu + \mathrm{i}(-\gamma - h). \tag{2.14}$$

Then (2.12) follows from [21, Theorem 5]. ∎

3. Computing the unknown function $S(t)$

Suppose that $S(t)$, $t \in J$, is the unknown function in connection of conformal mapping from Ω^- onto any of the canonical regions listed above. Let $\varphi(t)$ be the derivative of the unknown function $S(t)$ which shall be calculated by using the following theorem given in [20]. The proof of this theorem is reproduced for convenience.

Theorem 3.1. *Let $\upsilon, \varphi, \psi, \phi \in H$, $f(z)$ be analytic in Ω^- with $f(\infty) = 0$ and $g(z)$ be analytic in Ω^+ such that the boundary values of the functions f and g are given by*

$$\tilde{A}(t)f(\eta(t)) + \tilde{A}(t)g(\eta(t)) = \upsilon + \mathrm{i}\varphi, \tag{3.1}$$

where the function $\boldsymbol{J}\varphi$ is a given function defined as

$$\mathbf{J}\varphi = \tilde{h} = (\tilde{h}_1, \ldots, \tilde{h}_m). \tag{3.2}$$

Let also the boundary values of the function g satisfy

$$\tilde{A}(t)g(\eta(t)) = \psi + \mathrm{i}\phi. \tag{3.3}$$

Then the function φ is the unique solution of the integral equation

$$(\mathbf{I} + \mathbf{N}^* + \mathbf{J})\varphi = \mathbf{M}^*\upsilon + 2\phi + \tilde{h}. \tag{3.4}$$

Proof. It follows from (3.1) and from (3.3) the boundary values of the function f are given by

$$\tilde{A}(t)f(\eta(t)) = (\upsilon - \psi) + \mathrm{i}(\varphi - \phi). \tag{3.5}$$

Then, in view of (3.5), it follows from [22, Theorem 1] that the function $\varphi - \phi$ satisfies the integral equation

$$(\mathbf{I} + \mathbf{N}^*)(\varphi - \phi) = \mathbf{M}^*(\upsilon - \psi), \tag{3.6}$$

and from [33, Theorem 2(d)] that the function ϕ satisfies the integral equation

$$(\mathbf{I} - \mathbf{N}^*)\phi = -\mathbf{M}^*\psi. \tag{3.7}$$

Subtracting (3.7) form (3.6) yields the integral equation

$$(\mathbf{I} + \mathbf{N}^*)\varphi = 2\phi + \mathbf{M}^*\upsilon. \tag{3.8}$$

By adding (3.2) to (3.8), we obtain (3.4). ∎

For $j = 1, \ldots, m$, the functions $S_j(t)$ can be written as a summation of φ and ν_j,

$$S_j(t) = \int \varphi(t)dt + \nu_j = \rho_j(t) + \nu_j, \quad t \in J_j, \tag{3.9}$$

where ν_j are undetermined real constants and shall be calculated by Theorem 2.1. The derivative of the the unknown function $S(t)$i.e. $\varphi(t)$ is 2π-periodic. Thus, the function $\varphi(t)$ can be represented by a Fourier series

$$\varphi(t) = a_0^{[j]} + \sum_{k=1}^{\infty} a_k^{[j]} \cos kt + \sum_{k=1}^{\infty} b_k^{[j]} \sin kt, \quad t \in J_j. \tag{3.10}$$

Hence the functions $\rho_k(t)$ can be calculated by the Fourier series representation

$$\rho_j(t) = a_0^{[j]} t + \sum_{k=1}^{\infty} \frac{a_k^{[j]}}{k} \sin kt - \sum_{k=1}^{\infty} \frac{b_k^{[j]}}{k} \cos kt, \quad t \in J_j. \tag{3.11}$$

By obtaining $\rho(t)$ and $\nu(t)$, we can have $S(t)$ by (3.9).

4. An annulus with circular slits region

We assume that Φ maps the curve Γ_1 onto the unit circle $|w| = 1$, the curve Γ_m onto the circle $|w| = R_m$ and the curves Γ_j, $j = 2, 3, \ldots, m-1$, onto circular slits on the circles $|w| = R_j$, where $R_2, \ldots, R_m$ are undetermined real constants. The boundary values of the mapping function Φ are given by

$$\Phi(\eta(t)) = R(t) e^{\mathrm{i}S(t)}, \tag{4.1}$$

where $S(t)$ is the boundary correspondence function of $\Phi(\eta(t))$ and $R(t) = (1, R_2, \ldots, R_m)$. Thus, by taking logarithmic differentiation on both sides of (4.1), we get

$$\eta'(t) \frac{\Phi'(\eta(t))}{\Phi(\eta(t))} = \mathrm{i}S'(t). \tag{4.2}$$

The mapping function $\Phi(z)$ can be uniquely determined by assuming

$$c = \Phi(\infty) > 0, \tag{4.3}$$

where c is an undetermined positive real constant. Thus the mapping function $\Phi(z)$ can be expressed in the form

$$\Phi(z) = c \left(\frac{z - z_m}{z - z_1} \right) e^{F(z)}, \tag{4.4}$$

where z_1 is a fixed point in Γ_1, z_m is a fixed point in Γ_m and $F(z)$ is an analytic function with $F(\infty) = 0$. Hence by taking logarithm onto (4.4), we have

$$F(\eta(t)) + \ln c + \log \left(\frac{\eta(t) - z_m}{\eta(t) - z_1} \right) = \log(\Phi(\eta(t))). \tag{4.5}$$

In view of (2.8), (3.1) and (3.9), then it can be shown that (4.1) and (4.5) satisfy the boundary values (2.10) with

$$A(t) F(\eta(t)) = \gamma(t) + h(t) + \mathrm{i}[(\rho(t) + \mu(t)) + \nu(t)], \tag{4.6}$$

where

$$\begin{aligned} h(t) &= (\ln \frac{1}{c}, \ln \frac{R_2}{c}, \ldots, \ln \frac{R_m}{c}), \\ \nu(t) &= (c_1, c_2, \ldots, c_m), \end{aligned}$$

and the function $\gamma + \mathrm{i}\mu$ is defined by

$$\gamma(t) + \mathrm{i}\mu(t) = -\log \left(\frac{\eta(t) - z_m}{\eta(t) - z_1} \right). \tag{4.7}$$

Then, by Theorem 2.1, we can find the values h_j and ν_j. The piecewise real constants R_j can be calculated by

$$R_j = e^{h_j - h_1}. \tag{4.8}$$

Next, by differentiating both sides of (4.5) and using (4.2), we obtain

$$\eta'(t)F'(\eta(t))+\eta'(t)\left(\frac{1}{\eta(t)-z_m}-\frac{1}{\eta(t)-z_1}\right)=\mathrm{i}S'(t). \tag{4.9}$$

The function $f(z)$ defined in Ω^- by

$$f(z)=F'(z)+\frac{1}{z-z_m}-\frac{1}{z-z_1} \tag{4.10}$$

and the function $g(z)$ defined in Ω^+ with $g(z)=0$ satisfy the boundary values and assumptions in Theorem 3.1 with

$$\upsilon(t)=0 \quad \text{and} \quad \varphi(t)=S'(t). \tag{4.11}$$

Since the image of the curve Γ_1 is counterclockwise oriented, the image of the curve Γ_m is clockwise oriented and the images of the curves Γ_j, $j=2,\ldots,m-1$, are slits which are traversed-twice, we have $S_1(2\pi)-S_1(0)=2\pi$, $S_m(2\pi)-S_m(0)=-2\pi$ and $S_j(2\pi)-S_j(0)=0$. Hence the function $\tilde{h}(t)$ in (3.2) is given by

$$\tilde{h}(t)=\mathbf{J}\varphi=\mathbf{J}S'=(1,0,\ldots,-1). \tag{4.12}$$

Then, by Theorem 3.1, the function $S'(t)$ is the unique solution of the integral equation

$$(\mathbf{I}+\mathbf{N}^*+\mathbf{J})S'=\tilde{h}(t). \tag{4.13}$$

The function $S(t)$ is determined from $S'(t)$ and $\nu(t)$ by using the method described in Section 3. Hence, by obtaining all these information, the mapping function at the boundary points can be obtained by using (4.1). For computing the mapping functions of the interior points $z\in\Omega^-$, we have [13]

$$w=\Phi(z)=\Phi(\infty)+\frac{1}{2\pi\mathrm{i}}\int_\Gamma\frac{\Phi(\eta)}{\eta-z}d\eta=c+\frac{1}{2\pi\mathrm{i}}\int_J\frac{R(t)e^{\mathrm{i}S(t)}}{\eta(t)-z}\eta'(t)dt. \tag{4.14}$$

The function Φ^{-1} is analytic in the region U_a with a simple pole at $w=c$. Thus the function

$$\hat{\Phi}(w)=(w-c)\Phi^{-1}(w)$$

is analytic in U_a. Hence, by the Cauchy's integral formula, we have

$$z=\Phi^{-1}(w)=\frac{1}{w-c}\frac{1}{2\pi\mathrm{i}}\int_{\partial U_a}\frac{\xi-c}{\xi-w}\Phi^{-1}(\xi)d\xi. \tag{4.15}$$

By introducing $\xi(t)=R(S(t))e^{\mathrm{i}S(t)}$, we obtain

$$z=\Phi^{-1}(w)=\frac{1}{2\pi}\int_J\frac{1}{w-c}\frac{R(t)e^{\mathrm{i}S(t)}-c}{R(t)e^{\mathrm{i}S(t)}-w}\eta(t)R(t)e^{\mathrm{i}S(t)}S'(t)dt. \tag{4.16}$$

5. A disc with circular slits region

This canonical region is the interior of the unit circle along with $m-1$ circular arcs. We assume that Φ maps the curve Γ_1 onto the unit circle $|w|=1$ and the curves Γ_j, $j=2,\ldots,m$, onto circular slits on $|w|=R_j$, where $R_1,\ldots,R_m$ are undetermined real constants. This class of canonical region almost have the same geometrical meaning with the canonical region in Section 4, the only difference is that the inner circle in Section 4 will now become a circular slit. Then, the boundary values of the mapping function Φ are given by

$$\Phi(\eta(t))=R(t)e^{\mathrm{i}S(t)}, \tag{5.1}$$

where $S(t)$ is the boundary correspondence function and $R(t) = (1, R_2, \ldots, R_m)$. Thus, by logarithmic differentiation both sides of (5.1), we obtain

$$\eta'(t)\frac{\Phi'(\eta(t))}{\Phi(\eta(t))} = \mathrm{i}S'(t). \tag{5.2}$$

The mapping function $\Phi(z)$ can be uniquely determined by assuming

$$\Phi(\infty) = 0, \quad \lim_{z\to\infty} z\Phi(z) > 0. \tag{5.3}$$

Thus the mapping function $\Phi(z)$ can be expressed in the form

$$\Phi(z) = \frac{c}{z - z_1}\, e^{F(z)} \tag{5.4}$$

where $c = \lim_{z\to\infty} z\Phi(z)$ is an undetermined positive real constant and $F(z)$ is an analytic function with $F(\infty) = 0$. Hence

$$F(\eta(t)) + \ln c - \log(\eta(t) - z_1) = \log(\Phi(\eta(t))). \tag{5.5}$$

By using the same procedure as in previous section, we can show that (5.1) and (5.5) satisfy boundary values (2.10) with

$$A(t)F(\eta(t)) = \gamma(t) + h(t) + \mathrm{i}[(\rho(t) + \mu(t)) + \nu(t)], \tag{5.6}$$

where

$$\begin{aligned} h(t) &= (\ln\frac{1}{c}, \ln\frac{R_2}{c}, \ldots, \ln\frac{R_m}{c}), \\ \nu(t) &= (c_1, c_2, \ldots, c_m), \\ \gamma(t) + \mathrm{i}\mu(t) &= \log(\eta(t) - z_1). \end{aligned}$$

The values of h_j and ν_j can be obtained by using Theorem 2.1. Then, the values of R_j can be computed by

$$R_j = e^{h_j - h_1} \qquad \text{for} \quad j = 1, 2, \ldots, m.$$

To determine $S'(t)$, we begin by differentiating both sides of (5.5) and using (5.2), which yield

$$\eta'(t)F'(\eta(t)) - \eta'(t)\frac{1}{\eta(t) - z_1} = \mathrm{i}S'(t). \tag{5.7}$$

The function $f(z)$ defined in Ω^- by

$$f(z) = F'(z) - \frac{1}{z - z_1}, \tag{5.8}$$

and the function $g(z)$ defined in Ω^+ by $g(z) = 0$ satisfy the assumptions and the boundary values in Theorem 3.1 with

$$\upsilon(t) = 0 \quad \text{and} \quad \varphi(t) = S'(t). \tag{5.9}$$

Since the image of the curve Γ_1 is counterclockwise oriented and the images of the curves Γ_j, $j = 2, \ldots, m$, are traversed-twice slits so we have $S_1(2\pi) - S_1(0) = 2\pi$ and $S_j(2\pi) - S_j(0) = 0$. Hence the function $\tilde{h}(t)$ in (3.2) is given by

$$\tilde{h}(t) = \mathbf{J}\varphi = \mathbf{J}S' = (1, 0, \ldots, 0). \tag{5.10}$$

Then, by Theorem 3.1, the function $S'(t)$ is the unique solution of the integral equation

$$(\mathbf{I}+\mathbf{N}^*+\mathbf{J})S' = \tilde{h}(t). \tag{5.11}$$

For the $z \in \Omega^-$, by the Cauchy's integral formula, we have

$$w = \Phi(z) = \Phi(\infty) + \frac{1}{2\pi \mathrm{i}} \int_\Gamma \frac{\Phi(\eta)}{\eta - z} d\eta = \frac{1}{2\pi \mathrm{i}} \int_J \frac{R(t)e^{\mathrm{i}S(t)}}{\eta(t) - z} \eta'(t) dt. \tag{5.12}$$

To compute the inverse mapping function, note that Φ^{-1} is analytic in the region U_d with a simple pole at $w = 0$. Thus the function

$$\hat{\Phi}(w) = w\Phi^{-1}(w)$$

is analytic in U_d. Hence, by using the same procedure as in Section 4, we get

$$z = \Phi^{-1}(w) = \frac{1}{2\pi} \int_J \frac{1}{w} \frac{R(t)e^{\mathrm{i}S(t)}}{R(t)e^{\mathrm{i}S(t)} - w} \eta(t) R(t) e^{\mathrm{i}S(t)} S'(t) dt. \tag{5.13}$$

6. Circular slits region

This canonical region is the entire w-plane with m circular slits along the circles $|w| = R_k$ where $R_1, \ldots, R_m$ are undetermined real constants. Then, the boundary values of the mapping function Φ are given by

$$\Phi(\eta(t)) = R(t)e^{\mathrm{i}S(t)}, \tag{6.1}$$

where $S(t)$ is the boundary corresponding function and $R(t) = (R_1, \ldots, R_m)$. Thus, by logarithmic differentiation to both sides of (6.1), we obtain

$$\eta'(t) \frac{\Phi'(\eta(t))}{\Phi(\eta(t))} = \mathrm{i}S'(t). \tag{6.2}$$

The mapping function Φ can be uniquely determined by assuming

$$\Phi(\alpha) = 0, \quad \Phi(\infty) = \infty, \quad \lim_{z\to\infty} \frac{\Phi(z)}{z} = 1, \tag{6.3}$$

where α is a fixed point in Ω^-. Then Φ can be written as

$$\Phi(z) = (z - \alpha)\, e^{F(z)}, \tag{6.4}$$

where $F(z)$ is an analytic function with $F(\infty) = 0$. Hence

$$F(\eta(t)) + \log(\eta(t) - \alpha) = \log(\Phi(\eta(t))). \tag{6.5}$$

Equations (6.1) and (6.5) satisfy boundary values (2.10) with

$$A(t)F(\eta(t)) = \gamma(t) + h(t) + \mathrm{i}[(\rho(t) + \mu(t)) + \nu(t)], \tag{6.6}$$

where

$$\begin{aligned} h(t) &= (\ln R_0, \ln R_1, \ldots, \ln R_m), \\ \nu(t) &= (c_0, c_1, \ldots, c_m), \\ \gamma(t) + \mathrm{i}\mu(t) &= -\log(\eta(t) - \alpha). \end{aligned}$$

The values of h_j and ν_j can be obtained by using Theorem 2.1. Then, the values of R_j can be determined by

$$R_j = e^{h_j} \qquad \text{for} \quad j = 1, 2, \ldots, m.$$

Next, to find the values of the unknown functions $S'(t)$, by differentiating both sides of (6.5) and using (6.2), we have

$$\eta'(t)F'(\eta(t)) + \eta'(t)\frac{1}{\eta(t)-\alpha} = \mathrm{i}S'(t). \tag{6.7}$$

The function $f(z)$ defined in Ω^- by

$$f(z) = F'(z), \tag{6.8}$$

and the function $g(z)$ defined in Ω^+ by

$$g(z) = \frac{1}{z-\alpha}, \tag{6.9}$$

satisfy the assumptions and the boundary values in Theorem 3.1 with

$$\upsilon(t) = 0 \quad \text{and} \quad \varphi(t) = S'(t). \tag{6.10}$$

Since the image of the curves Γ_j, $j = 1,\ldots,m$ are traversed-twice circular slits, we have $S_j(2\pi) - S_j(0) = 0$. Hence the function $\tilde{h}(t)$ in (3.2) is given by

$$\tilde{h}(t) = \mathbf{J}\varphi = \mathbf{J}S' = (0,0,\ldots,0). \tag{6.11}$$

Then, by Theorem 3.1, the function $S'(t)$ is the unique solution of the integral equation

$$(\mathbf{I} + \mathbf{N}^* + \mathbf{J})S' = 2\phi, \tag{6.12}$$

where

$$\phi(t) = \mathrm{Im}[\tilde{A}(t)g(\eta(t))] = \mathrm{Im}\left[\eta'(t)\frac{1}{\eta(t)-\alpha}\right].$$

From [34, p. 112], $\Phi(z)$ has the Laurent series expansion near $z = \infty$ as

$$\Phi(z) = z + a_0 + \frac{a_1}{z} + \frac{a_2}{z^2} + \cdots.$$

For computing the mapping function of the interior points $z \in \Omega^-$, let $\hat{\Phi}(z)$ be an analytic function for $z \in \Omega^-$ and be defined as

$$\hat{\Phi}(z) = \frac{\Phi(z)}{z-\alpha}, \qquad \text{where} \quad \lim_{z\to\infty}\hat{\Phi}(z) = 1.$$

Then by the Cauchy's integral formula [13] we have

$$w = z - \alpha + \frac{(z-\alpha)}{2\pi\mathrm{i}}\int_J \frac{\Phi(\eta(t))}{(\eta(t)-\alpha)(\eta(t)-z)}\eta'(t)dt. \tag{6.13}$$

For computing the inverse maps, note that the inverse of Laurent series expansion for $\Phi^{-1}(z)$ near ∞ has the following representation [34, p. 114]

$$\Phi^{-1}(w) = w + b_0 + \frac{b_1}{w} + \frac{b_2}{w^2} + \cdots.$$

The function $G(w)$ defined on U_c by

$$G(w) = \frac{\Phi^{-1}(w) - \alpha}{w}$$

is analytic in U_c with $G(\infty) = 1$. Then by the Cauchy's integral formula, we have

$$G(w) = G(\infty) + \frac{1}{2\pi\mathrm{i}}\int_{\partial U_c}\frac{G(\zeta)}{\zeta - w}d\zeta.$$

By introducing $\zeta(t) = \Phi(\eta(t))$, we obtain for $z \in \Omega^-$ by

$$\frac{z-\alpha}{w} = 1 + \frac{1}{2\pi \mathrm{i}} \int_J \frac{\Phi^{-1}(\Phi(\eta(t)) - \alpha}{\Phi(\eta(t))(\Phi(\eta(t)) - w)} R(t) e^{\mathrm{i}S(t)} \mathrm{i} S'(t) dt,$$

which implies

$$z = w + \alpha + \frac{w}{2\pi \mathrm{i}} \int_J \frac{\eta(t) - \alpha}{\Phi(\eta(t))(\Phi(\eta(t)) - w)} R(t) e^{\mathrm{i}S(t)} \mathrm{i} S'(t) dt.$$

7. Radial slits region

This canonical region is the entire w-plane with m radial slits along the rays $\arg(w) = R_k$, where R_k, $k = 1, \ldots, m$, are undetermined piecewise real constants and $S(t)$ is the unknown function. The boundary values of the mapping function Φ are given by

$$\Phi(\eta(t)) = e^{S(t)} e^{\mathrm{i}R(t)}. \tag{7.1}$$

Thus, by taking logarithmic differentiation on both sides of (7.1), we have

$$\eta'(t) \frac{\Phi'(\eta(t))}{\Phi(\eta(t))} = S'(t). \tag{7.2}$$

The mapping function Φ can be uniquely determined by assuming

$$\Phi(\alpha) = 0, \quad \Phi(\infty) = \infty, \quad \lim_{z \to \infty} \frac{\Phi(z)}{z} = 1, \tag{7.3}$$

where α is a fixed point in Ω^-. Then Φ can be written as

$$\Phi(z) = (z - \alpha) e^{\mathrm{i}F(z)}, \tag{7.4}$$

where $F(z)$ is an analytic function with $F(\infty) = 0$. Hence by taking logarithm to both sides of (7.4), we get

$$-F(\eta(t)) + \mathrm{i} \log(\eta(t) - \alpha) = \mathrm{i} \log(\Phi(\eta(t))). \tag{7.5}$$

Hence (7.1) and (7.5) satisfy the boundary values (2.10) with

$$A(t) F(\eta(t)) = \gamma(t) + h(t) + \mathrm{i}[(-\rho(t) + \mu(t)) + \nu(t)], \tag{7.6}$$

where

$$\begin{aligned} h(t) &= (R_1, \ldots, R_m), \\ \nu(t) &= (-c_1, \ldots, -c_m), \\ \gamma(t) + \mathrm{i}\mu(t) &= \mathrm{i} \log(\eta(t) - \alpha). \end{aligned}$$

Then, by differentiating both sides of (7.4) and using (7.2), we get

$$\eta'(t)(-F'(\eta(t))) + \eta'(t) \frac{\mathrm{i}}{\eta(t) - \alpha} = \mathrm{i} S'(t). \tag{7.7}$$

The function $f(z)$ defined in Ω^- by

$$f(z) = -F'(z) \tag{7.8}$$

and the function $g(z)$ defined in Ω^+ by

$$g(z) = \frac{\mathrm{i}}{z - \alpha} \tag{7.9}$$

satisfy the assumptions and the boundary values in Theorem 3.1 with

$$\upsilon(t) = 0 \quad \text{and} \quad \varphi(t) = S'(t). \tag{7.10}$$

Since the images of the curves Γ_j, $j = 1,\ldots,m$, are traversed-twice radial slits, we have $S_j(2\pi) - S_j(0) = 0$. Hence the function $\tilde{h}(t)$ in (3.2) is given by

$$\tilde{h}(t) = \mathbf{J}\varphi = \mathbf{J}S' = (0,0,\ldots,0). \tag{7.11}$$

Then, by Theorem 3.1, the function $S'(t)$ is the unique solution of the integral equation

$$(\mathbf{I} + \mathbf{N}^* + \mathbf{J})S' = 2\phi, \tag{7.12}$$

where

$$\phi(t) = \mathrm{Im}[\tilde{A}(t)g(\eta(t))] = \mathrm{Im}\left[\eta'(t)\frac{\mathrm{i}}{\eta(t)-\alpha}\right].$$

For approximating the mapping at the interior points, notice that $\Phi(z)$ has the Laurent series expansion near $z = \infty$ as [34, p. 112]

$$\Phi(z) = z + a_0 + \frac{a_1}{z} + \frac{a_2}{z^2} + \cdots.$$

Let $\hat{\Phi}(z)$ be an analytic function for $z \in \Omega^-$ defined as

$$\hat{\Phi}(z) = \frac{\Phi(z)}{z-\alpha}, \qquad \text{where} \quad \lim_{z\to\infty}\hat{\Phi}(z) = 1.$$

Then by the Cauchy's integral formula [13], we have

$$w = z - \alpha + \frac{(z-\alpha)}{2\pi\mathrm{i}}\int_J \frac{\Phi(\eta(t))}{(\eta(t)-\alpha)(\eta(t)-z)}\eta'(t)dt. \tag{7.13}$$

For computing the inverse mapping function, observe that the inverse of Laurent series expansion for $\Phi(z)$ near ∞ has the following representation [34, p. 114]

$$\Phi^{-1}(w) = w + b_0 + \frac{b_1}{w} + \frac{b_2}{w^2} + \cdots.$$

Let $G(w)$ be an analytic function for $w \in U_c$ defined as

$$G(w) = \frac{\Phi^{-1}(w)-\alpha}{w}, \qquad \text{where} \quad \lim_{w\to\infty} G(w) = 1.$$

Then, by using the same reasoning as in Section 6, we get

$$z = w + \alpha + \frac{w}{2\pi\mathrm{i}}\int_J \frac{\eta(t)-\alpha}{\Phi(\eta(t))(\Phi(\eta(t))-w)}S'(t)e^{S(t)\mathrm{i}R(t)}dt.$$

8. Parallel slits region

This canonical region is the entire w-plane with m parallel slits on the straight lines

$$\mathrm{Re}\left[e^{\mathrm{i}(\pi/2-\theta)}w\right] = R_j, \quad j = 1,\ldots,m, \tag{8.1}$$

where $R_1,\ldots,R_m$ are undetermined real constants and θ is the given angle of intersection between the lines (8.1) and the real axis. The boundary values of the mapping function Φ satisfy

$$e^{\mathrm{i}(\pi/2-\theta)}\Phi(\eta(t)) = R(t) + \mathrm{i}S(t), \tag{8.2}$$

where $S(t)$ is the unknown function and $R(t) = (R_1, \ldots, R_m)$ is a piecewise real constant function. Thus, by logarithmic differentiation to both sides of (8.2), we get

$$e^{\mathrm{i}(\pi/2-\theta)}\eta'(t)\Phi'(\eta(t)) = \mathrm{i}S'(t). \tag{8.3}$$

The mapping function Φ is uniquely determined by the normalization

$$\Phi(\infty) = \infty, \quad \lim_{z\to\infty}(\Phi(z) - z) = 0. \tag{8.4}$$

Thus, the function Φ can be written as

$$\Phi(z) = z + e^{-\mathrm{i}(\pi/2-\theta)}F(z), \tag{8.5}$$

where $F(z)$ is an analytic function with $F(\infty) = 0$. Hence

$$F(\eta(t)) + e^{\mathrm{i}(\pi/2-\theta)}\eta(t) = e^{\mathrm{i}(\pi/2-\theta)}\Phi(\eta(t)). \tag{8.6}$$

Then (8.2) and (8.6) satisfy boundary values (2.10) with

$$A(t)F(\eta(t)) = \gamma(t) + h(t) + \mathrm{i}[(\rho(t) + \mu(t)) + \nu(t)], \tag{8.7}$$

where

$$\begin{aligned} h(t) &= (R_1, \ldots, R_m), \\ \nu(t) &= (c_1, \ldots, c_m), \\ \gamma(t) + \mathrm{i}\mu(t) &= -e^{\mathrm{i}(\pi/2-S)}\eta(t). \end{aligned}$$

Next, by differentiating both sides of (8.6) and using (8.3), we have

$$\eta'(t)F'(\eta(t)) + \eta'(t)e^{\mathrm{i}(\pi/2-\theta)} = \mathrm{i}S'(t). \tag{8.8}$$

The function $f(z)$ defined in Ω^- by

$$f(z) = F'(z) \tag{8.9}$$

and the function $g(z)$ defined in Ω^+ by

$$g(z) = e^{\mathrm{i}(\pi/2-\theta)} \tag{8.10}$$

satisfy the assumptions and the boundary values in Theorem 3.1 with

$$\upsilon(t) = 0 \quad \text{and} \quad \varphi(t) = S'(t). \tag{8.11}$$

Since the images of the curves Γ_j, $j = 1, \ldots, m$, are traversed-twice parallel slits, we have $S_j(2\pi) - S_j(0) = 0$. Hence the function $\tilde{h}(t)$ in (3.2) is given by

$$\tilde{h}(t) = \mathbf{J}\varphi = \mathbf{J}S' = (0, 0, \ldots, 0). \tag{8.12}$$

Then, by Theorem 3.1, the function $S'(t)$ is the unique solution of the integral equation

$$(\mathbf{I} + \mathbf{N}^* + \mathbf{J})S' = 2\phi, \tag{8.13}$$

where

$$\phi(t) = \mathrm{Im}[\tilde{A}(t)g(\eta(t))] = \mathrm{Im}\left[\eta'(t)e^{\mathrm{i}(\pi/2-\theta)}\right].$$

By obtaining all the information above, the boundary values of the mapping function can be calculated by

$$\Phi(\eta) = e^{-\mathrm{i}(\pi/2-\theta)}(R(t) + \mathrm{i}S(t)).$$

From [34, p. 102], $\Phi(z)$ has the Laurent expansion series near ∞ as

$$\Phi(z) = z + \frac{a_1}{z} + \frac{a_2}{z^2} + \frac{a_3}{z^3} + \cdots.$$

Let $\hat{\Phi}(z)$ be an analytic function for $z \in \Omega^-$ defined as

$$\hat{\Phi}(z) = \Phi(z) - z, \qquad \text{where} \quad \lim_{z\to\infty} \hat{\Phi}(z) = 0.$$

Then by the Cauchy's integral formula [13], we have

$$w = z + \frac{1}{2\pi \mathrm{i}} \int_J \frac{\Phi(\eta(t)) - \eta(t)}{\eta(t) - z} \eta'(t) dt. \tag{8.14}$$

For approximating the inverse mapping function, the inverse of Laurent series expansion for $\Phi(z)$ near ∞ has the following representation [34, p. 114]

$$\Phi^{-1}(w) = w + \frac{b_1}{w} + \frac{b_2}{w^2} + \frac{b_3}{w^3} + \cdots.$$

Let $G(w)$ be an analytic function in U_p be defined as

$$G(w) = \Phi^{-1}(w) - w, \qquad \text{where} \quad \lim_{w\to\infty} G(w) = 0.$$

Then by using the same procedure as in previous section, we have

$$z = w + \frac{1}{2\pi \mathrm{i}} \int_J \frac{\eta(t) - \Phi(\eta(t))}{\Phi(\eta(t)) - w} e^{-\mathrm{i}(\pi/2-\theta)} \mathrm{i} S'(t) dt.$$

9. Numerical examples

Since the boundaries Γ_j are parameterized by $\eta_j(t)$ which are 2π-periodic functions, the reliable method to solve the integral equations are by means of Nyström method with trapezoidal rule [4]. Each boundary will be discretized by n number of equidistant points. For region that contains corner points, the integral equation need to be modified slightly, the computational details are similar to [23]. The resulting linear system is then solved by using Gaussian elimination method (see [17, 18] for more details).

In this paper, we choose test regions with connectivities three and four. The computations were carried out on Intel processor Quad-core 2.33GHz, 4-gb DDR3 RAM using algorithms coded in MATLAB R2011a.

Example 9.1. Consider an unbounded region Ω^- bounded by three circles

$$\begin{aligned}
\Gamma_1(t) &= \ \ 2 + e^{-\mathrm{i}t}, && 0 \le t \le 2\pi, \\
\Gamma_2(t) &= -1 + \mathrm{i}\sqrt{3} + 0.5e^{-\mathrm{i}t}, && 0 \le t \le 2\pi, \\
\Gamma_3(t) &= -1 - \mathrm{i}\sqrt{3} + 1.5e^{-\mathrm{i}t}, && 0 \le t \le 2\pi.
\end{aligned}$$

For this example, the special points are $z_1 = 2, z_3 = -1 - \mathrm{i}\sqrt{3}$, and $\alpha = 0$. Table 1 shows the approximated values for conformal moduli for each canonical region with $n = 512$. Figure 2 shows the images of conformal mapping of Ω^- onto five classes of canonical regions for $n = 512$. It is not possible to show the image of the whole original region Ω^- since it is unbounded. So, we have restricted the region Ω^- for only the points $z = x + iy$ which satisfy $|x| \le 5.5$ and $|y| \le 4$. The clover-like shapes "holes" in the 2nd and 3rd images in Figure 2 are due to the images of points $z \in \Omega^-$ that have not been computed, i.e., the points $z = x + \mathrm{i}y \in \Omega^-$ which satisfy $|x| > 5.5$ and $|y| > 4$. This example has

been considered in [17, 35] and [1] for U^c and U^d. Table 2 and Table 3 show the error norm for the boundary values $\max_{1\leq j\leq 3}||w_j - \hat{w_j}||_\infty$ between our method, [17] and [35]. Since [35] considered exterior unit disk with circular slits as the canonical region, we need to change their boundary values by $1/|\Phi(z)|$. Table 4 shows the time comparison between our presented method with [17,35]. For U_d, we didn't compare the time taken for computing the conformal mapping with [35] as they used different type of canonical region. From Table 1 to Table 4, we can conclude that our presented method is accurate, fast and reliable. Figures 3–7 show the inverse transformation for each canonical regions.

Table 1. The values of approximated conformal moduli in Example 1.

j	U_a	U_d	U_c
1	1.000000000000000	1.000000000000000	2.695852404127037
2	0.351592984957793	0.337011016555280	2.912178845710424
3	0.179209929196331	0.366977372407806	2.265373694952072
j	U_r	U_p	
1	−0.235829740944631	−0.326576617247789	
2	2.246730512278837	0.996414684417039	
3	−2.005025892943342	−1.478338658064248	

Table 2. Error norm $\max\limits_{1\leq j\leq 3}||w_j - \hat{w_j}||_\infty$ of our method with [17] for Example 1.

n	U_a	U_d	U_c	U_r	$U_{p,\pi/2}$
32	5.208×10^{-07}	4.264×10^{-07}	0.0134	0.0022	4.076×10^{-06}
64	2.378×10^{-12}	2.401×10^{-12}	5.219×10^{-05}	8.841×10^{-06}	1.528×10^{-11}
128	8.551×10^{-15}	5.575×10^{-15}	2.469×10^{-09}	4.112×10^{-10}	1.493×10^{-14}
256	1.601×10^{-14}	1.113×10^{-14}	5.795×10^{-14}	1.194×10^{-13}	3.688×10^{-14}

Table 3. Error norm $\max\limits_{1\leq j\leq 3}||w_j - \hat{w_j}||_\infty$ of our method with [35] for Example 1.

n	U_a	U_d	U_c	U_r	$U_{p,\pi/2}$
32	5.588×10^{-07}	5.032×10^{-07}	0.2969	0.1635	4.103×10^{-06}
64	2.408×10^{-12}	2.461×10^{-12}	9.342×10^{-05}	2.045×10^{-05}	1.528×10^{-11}
128	8.705×10^{-14}	3.959×10^{-14}	4.680×10^{-09}	8.259×10^{-10}	2.336×10^{-12}
256	3.833×10^{-13}	1.755×10^{-13}	2.423×10^{-12}	5.394×10^{-13}	7.631×10^{-12}

Table 4. Time taken in seconds for computing the conformal mapping onto the canonical regions for Example 1.

n	Methods	U_a	U_d	U_c	U_r	$U_{p,\pi/2}$
128	Ours	1.115626 s	1.123708 s	1.103998 s	1.333334 s	1.325958 s
	Arif *et al.* [35]	2.146316 s	− − −	1.405052 s	2.525786 s	2.177692 s
	Nasser [17]	2.738256 s	2.701307 s	2.727848 s	2.937508 s	2.913769 s
256	Ours	2.076334 s	2.071060 s	2.072290 s	2.388166 s	2.388353 s
	Arif *et al.* [35]	10.539557 s	− − −	4.427757 s	8.874106 s	7.293674 s
	Nasser [17]	9.647205 s	9.528054 s	9.660037 s	9.920425 s	9.961381 s
512	Ours	4.540774 s	4.558842 s	4.536835 s	5.122694 s	5.173554 s
	Arif *et al.* [35]	91.799515 s	− − −	20.95380 s	49.43904 s	34.80111 s
	Nasser [17]	42.275036 s	41.09918 s	42.65789 s	43.37522 s	42.53321 s
1024	Ours	12.671643 s	12.735873 s	12.688997 s	13.79570 s	13.69144 s
	Arif *et al.* [35]	1942.2733 s	− − −	168.19319 s	293.1323 s	249.0591 s
	Nasser [17]	315.9718 s	269.74096 s	293.71689 s	247.7996 s	286.0053 s

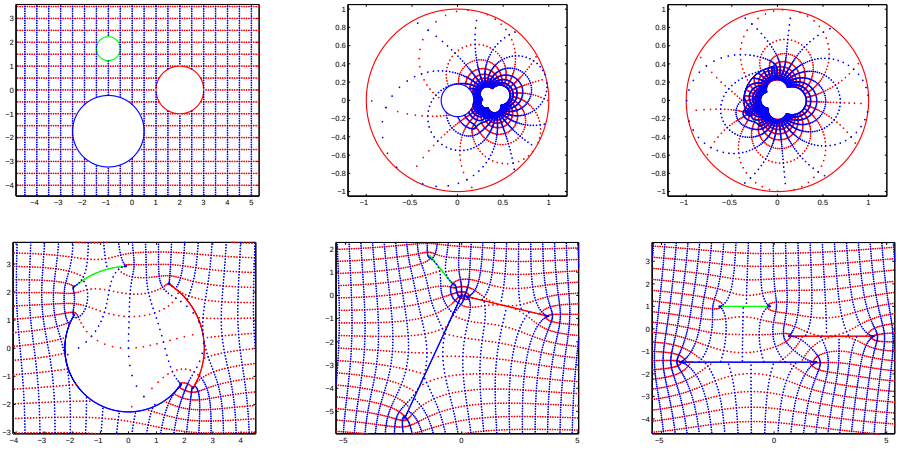

Figure 2. The original region Ω^- and its canonical images with $\theta = \pi$ for the parallel slits region,

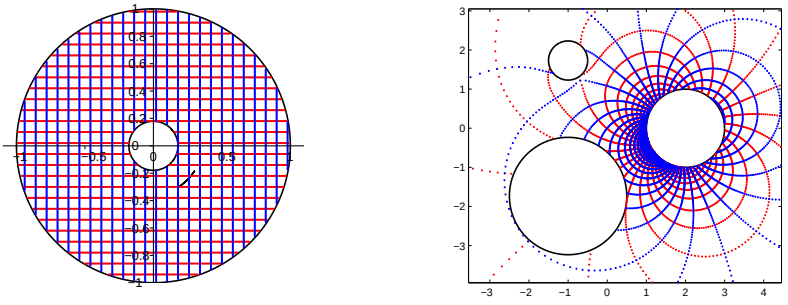

Figure 3. The inverse image of the annulus with circular slits region.

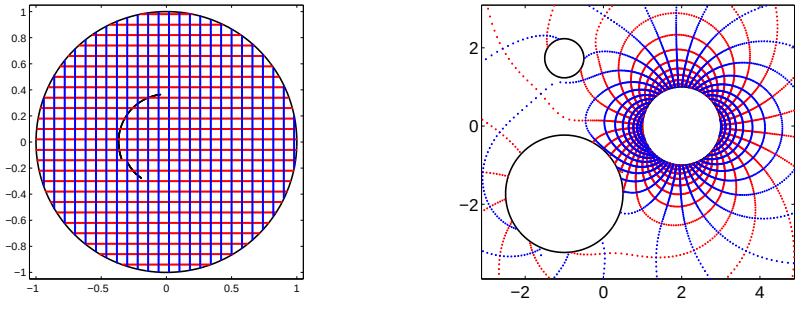

Figure 4. The inverse image of the disk with circular slits region.

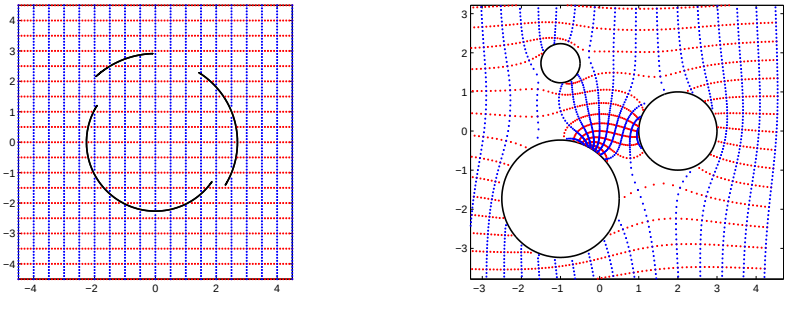

Figure 5. The inverse image of the circular slits region.

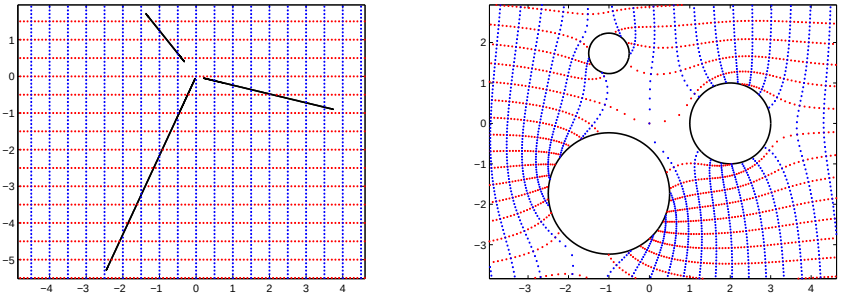

Figure 6. The inverse image of the radial slits region.

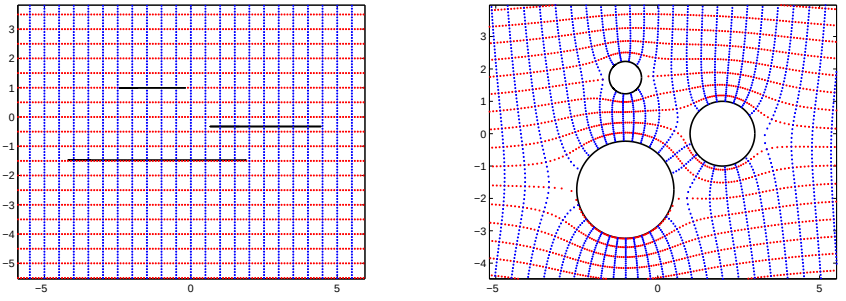

Figure 7. The inverse image of the parallel slits region.

Example 9.2. Consider an unbounded region Ω^- bounded by four rectangles

$$\begin{aligned}
\Gamma_1(t) &= \{x+\mathrm{i}y : |x-2| \leqslant 1, |y-1| \leqslant 1\},\\
\Gamma_2(t) &= \{x+\mathrm{i}y : |x-2| \leqslant 1, |y+2| \leqslant 1\},\\
\Gamma_3(t) &= \{x+\mathrm{i}y : |x+3| \leqslant 2, |y+2| \leqslant 1\},\\
\Gamma_4(t) &= \{x+\mathrm{i}y : |x+3| \leqslant 2, |y-1| \leqslant 1\}.
\end{aligned}$$

The conformal mapping for this example is closely related to the Schwarz-Christoffel mapping. The special points are $z_1 = 2+\mathrm{i}, z_4 = -3+\mathrm{i}$, and $\alpha = 0$. Figure 8 shows the images of the conformal mapping of unbounded quadruply connected region onto the classes of canonical slit regions for $n = 512$. The reasons for the appearances of the clover-like shapes "holes" in the 2nd and 3rd images in Figure 8 are the same as in the 2nd and 3rd images in Figure 2. The values for approximated conformal moduli are shown in Table 5 for $n = 1024$. Table 6 shows the time taken for computing the conformal maps onto its canonical regions. Figures 9–13 shows the images of inverse transformation for each canonical region onto the original region.

Table 5. The values of approximated conformal moduli in Example 2.

j	U^a	U^d	U^c
1	1.000000000000000	1.000000000000000	3.344702632925646
2	0.517512691928356	0.479372261123766	3.961983593647091
3	0.215953410129373	0.304215660437710	4.175190764006607
4	0.142159202935490	0.328418971877769	3.705458446175335
j	U^r	$U^p_{\pi/3}$	
1	0.363896619147592	0.569192974854135	
2	−0.719493954812626	1.406334127895268	
3	−2.625093020158977	−1.527412741498223	
4	2.910015395960396	−2.299593756387775	

Table 6. Time taken in seconds for computing the conformal mapping onto the canonical regions for Example 2.

n	U^a	U^d	U^c	U^r	$U^p_{\pi/3}$
128	1.541186 s	1.499868 s	1.521170 s	1.535602 s	1.533885 s
256	3.013458 s	2.982456 s	2.975827 s	2.992448 s	2.989267 s
512	6.993330 s	6.932142 s	6.918470 s	6.934293 s	6.940827 s
1024	21.45491 s	21.43855 s	21.06668 s	21.12070 s	21.14749 s

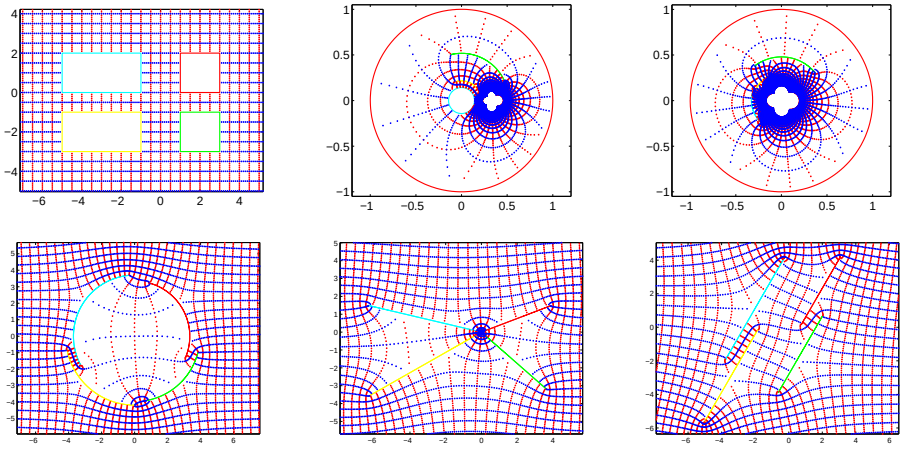

Figure 8. The original region Ω^- and its canonical images with $\theta = \pi/3$ for the parallel slits region.

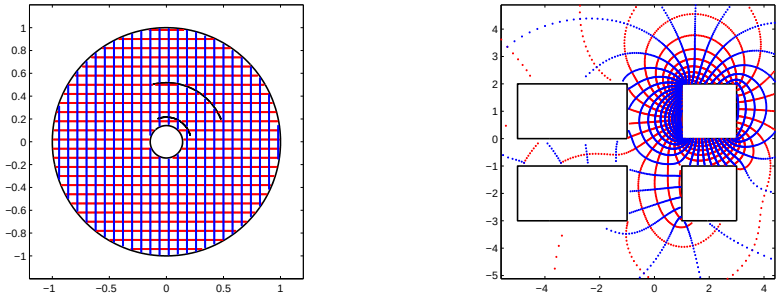

Figure 9. The inverse image of the annulus with circular slits region.

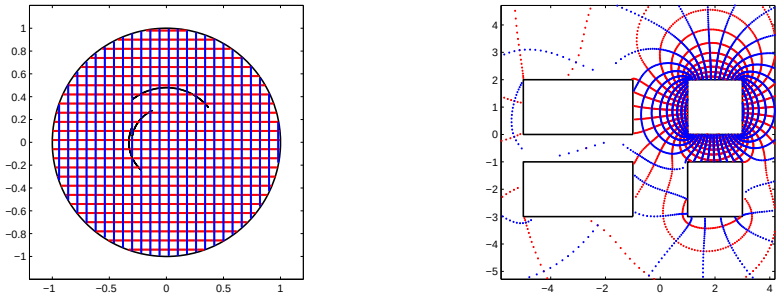

Figure 10. The inverse image of the disk with circular slits region.

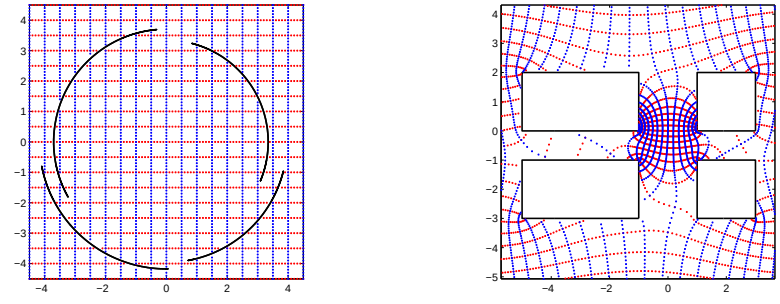

Figure 11. The inverse image of the circular slits region.

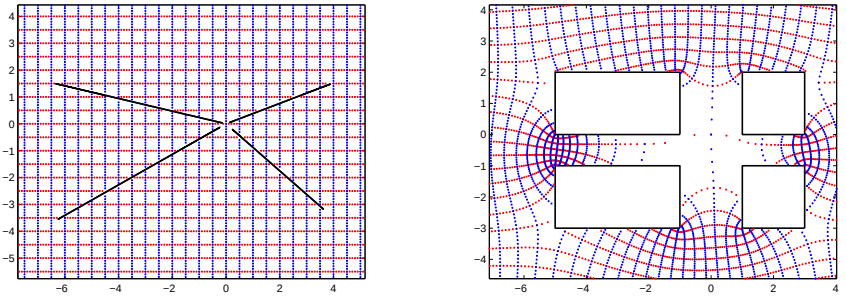

Figure 12. The inverse image of the radial slits region.

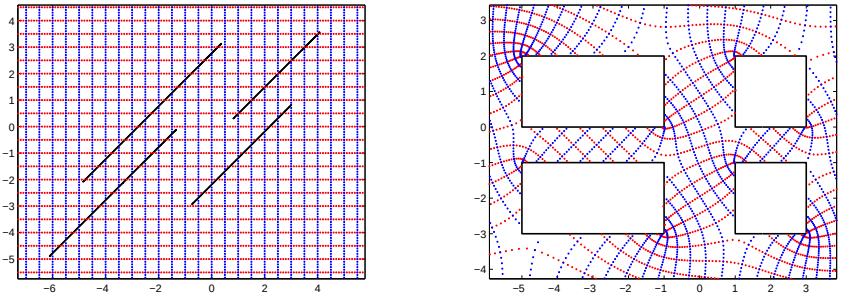

Figure 13. The inverse image of the parallel slits region.

10. Conclusion

In this paper, we have constructed a unified method for numerical conformal mappings of unbounded multiply connected regions onto canonical slit regions. The advantages of the presented method is that it can be used to compute the conformal mapping function as well as its inverse. The presented method can be used even if the boundary of the original region Ω^- is a piecewise smooth boundary.

Table 4 and Table 6 show that as the number of connectivity of unbounded region Ω^- increase, the time taken for computing the conformal maps onto its canonical regions also increase. Hence, solving the linear system obtained by discretizing our integral equations by a fast method is certainly recommended for regions with high connectivity or when the boundary components Γ_j lie closed to each other where more discretization points are needed. Since the kernels of the integral equation are the adjoint of the generalized Neumann kernel used in [19], the fast method used in [19] can be used to solve the boundary integral equation with the adjoint generalized Neumann kernel presented in this paper.

Acknowledgement. This work was supported in part by the Malaysian Ministry of Higher Education (MOHE) through the Research Management Centre (RMC), Universiti Teknologi Malaysia (GUP Q.J130000.2526.04H62). The authors would like to thank the anonymous

referees for their valuable comments and suggestions on the manuscript which improved the presentation of the paper.

References

[1] K. Amano, A charge simulation method for numerical conformal mapping onto circular and radial slit domains, *SIAM J. Sci. Comput.* **19** (1998), no. 4, 1169–1187 (electronic).

[2] K. Amano, D. Okano, H. Ogata and M. Sugihara, Numerical conformal mappings of unbounded multiply-connected domains using the charge simulation method, *Bull. Malays. Math. Sci. Soc. (2)* **26** (2003), no. 1, 35–51.

[3] V. V. Andreev, D. Daniel and T. H. McNicholl, Technical report: Computation on the extended complex plane and conformal mapping of multiply-connected domains, in *Proceedings of the Fifth International Conference on Computability and Complexity in Analysis (CCA 2008)*, 127–139, Electron. Notes Theor. Comput. Sci., 221 Elsevier Sci. B. V., Amsterdam.

[4] K. E. Atkinson, *The Numerical Solution of Integral Equations of the Second Kind*, Cambridge Monographs on Applied and Computational Mathematics, 4, Cambridge Univ. Press, Cambridge, 1997.

[5] N. Benchama and T. K. DeLillo, A brief overview of Fornberg-like methods for conformal mapping of simply and multiply connected regions, *Bull. Malays. Math. Sci. Soc. (2)* **26** (2003), no. 1, 53–62.

[6] N. Benchama, T. K. DeLillo, T. Hrycak and L. Wang, A simplified Fornberg-like method for the conformal mapping of multiply connected regions comparisons and crowding, *J. Comput. Appl. Math*. **209** (2007), no. 1, 1–21.

[7] D. Crowdy, Conformal slit maps in applied mathematics, *ANZIAM J.* **53** (2012), 171-189.

[8] D. Crowdy, The Schwarz-Christoffel mapping to bounded multiply connected polygonal domains, *Proc. R. Soc. Lond. Ser. A Math. Phys. Eng. Sci.* **461** (2005), no. 2061, 2653–2678.

[9] D. Crowdy and J. Marshall, Conformal mappings between canonical multiply connected domains, *Comput. Methods Funct. Theory* **6** (2006), no. 1, 59–76.

[10] R. Czapla, V. Mityushev and N. Rylko, Conformal mapping of circular multiply connected domains onto slit domains, *Electron. Trans. Numer. Anal.* **39** (2012), 286–297.

[11] T. K. DeLillo, M. A. Horn and J. A. Pfaltzgraff, Numerical conformal mapping of multiply connected regions by Fornberg-like methods, *Numer. Math.* **83** (1999), no. 2, 205–230.

[12] B. Fornberg, A numerical method for conformal mappings, *SIAM J. Sci. Statist. Comput.* **1** (1980), no. 3, 386–400.

[13] F. D. Gakhov, *Boundary Value Problems*, Translation edited by I. N. Sneddon, Pergamon, Oxford, 1966.

[14] P. Henrici, *Applied and Computational Complex Analysis, Vol. 3*, Pure and Applied Mathematics (New York), Wiley, New York, 1986.

[15] P. Koebe, Abhandlungen zur Theorie der konformen Abbildung, *Acta Math.* **41** (1916), no. 1, 305–344.

[16] A. H. M. Murid and L.-N. Hu, Numerical experiment on conformal mapping of doubly connected regions onto a disk with a slit, *Int. J. Pure Appl. Math.* **51** (2009), no. 4, 589–608.

[17] M. M. S. Nasser, Numerical conformal mapping via a boundary integral equation with the generalized Neumann kernel, *SIAM J. Sci. Comput.* **31** (2009), no. 3, 1695–1715.

[18] M. M. S. Nasser, A boundary integral equation for conformal mapping of bounded multiply connected regions, *Comput. Methods Funct. Theory* **9** (2009), no. 1, 127–143.

[19] M. M. S. Nasser and F. A. A. Al-Shihri, A fast boundary integral method for conformal mapping of multiply connected regions, *SIAM J. Sci. Comput.* **35** (2013), no. 3, A1736–A1760.

[20] M. M. S. Nasser, A. H. M. Murid and A. W. K. Sangawi, Numerical conformal mapping via a boundary integral equation with the adjoint generalized Neumann kernel, preprint.

[21] M. M. S. Nasser, A. H. M. Murid, M. Ismail and E. M. A. Alejaily, Boundary integral equations with the generalized Neumann kernel for Laplace's equation in multiply connected regions, *Appl. Math. Comput.* **217** (2011), no. 9, 4710–4727.

[22] M. M. S. Nasser, The Riemann-Hilbert problem and the generalized Neumann kernel on unbounded multiply connected regions, *The University Researcher Journal* **20** (2009), 47–60.

[23] M. M. S. Nasser, A. H. M. Murid and Z. Zamzamir, A boundary integral method for the Riemann-Hilbert problem in domains with corners, *Complex Var. Elliptic Equ.* **53** (2008), no. 11, 989–1008.

[24] Z. Nehari, *Conformal Mapping*, McGraw-Hill, Inc., New York, Toronto, London, 1952.

[25] A. W. K. Sangawi, A. H. M. Murid and M. M. S. Nasser, Linear integral equations for conformal mapping of bounded multiply connected regions onto a disk with circular slits, *Appl. Math. Comput.* **218** (2011), no. 5, 2055–2068.

[26] A. W. K. Sangawi, A. H. M. Murid and M. M. S. Nasser, Parallel slits map of bounded multiply connected regions, *J. Math. Anal. Appl.* **389** (2012), no. 2, 1280–1290.

[27] A. W. K. Sangawi, A. H. M. Murid and M. M. S. Nasser, Annulus with circular slit map of bounded multiply connected regions via integral equation method, *Bull. Malays. Math. Sci. Soc. (2)* **35** (2012), no. 4, 945–959.

[28] A. W. K. Sangawi, A. H. M. Murid and M. M. S. Nasser, Circular slits map of bounded multiply connected regions, *Abstr. Appl. Anal.* **2012**, Art. ID 970928, 26 pp.

[29] A. W. K. Sangawi, A. H. M. Murid and M. M. S. Nasser, Radial slit maps of bounded multiply connected regions, *J. Sci. Comput.* **55** (2013), no. 2, 309–326.

[30] L. N. Trefethen, ed., *Numerical Conformal Mapping*, North-Holland, Amsterdam, 1986.

[31] R. Wegmann, Fast conformal mapping of multiply connected regions, *J. Comput. Appl. Math.* **130** (2001), no. 1-2, 119–138.

[32] R. Wegmann, Methods for numerical conformal mapping, in *Handbook of Complex Analysis: Geometric Function Theory. Vol. 2*, 351–477, Elsevier, Amsterdam, 2005.

[33] R. Wegmann and M. M. S. Nasser, The Riemann-Hilbert problem and the generalized Neumann kernel on multiply connected regions, *J. Comput. Appl. Math.* **214** (2008), no. 1, 36–57.

[34] G. C. Wen, *Conformal Mappings and Boundary Value Problems*, translated from the Chinese by Kuniko Weltin, Translations of Mathematical Monographs, 106, Amer. Math. Soc., Providence, RI, 1992.

[35] A. A. M. Yunus, A. H. M. Murid and M. M. S. Nasser, Conformal mapping of unbounded multiply connected regions onto canonical slit regions, *Abstr. Appl. Anal.* **2012**, Art. ID 293765, 29 pp.